

Smooth Densities and Generative Modeling with Unsupervised Random Forests

David S. Watson^{1*}, Kristin Blesch^{2,3}, Jan Kapar^{2,3}, Marvin N. Wright^{2,3,4}

¹Department of Statistical Science, University College London, London, UK

²Leibniz Institute for Prevention Research & Epidemiology – BIPS, Bremen, Germany

³Faculty of Mathematics and Computer Science, University of Bremen, Bremen, Germany

⁴Department of Public Health, University of Copenhagen, Copenhagen, Denmark

*Corresponding author: David S. Watson; david.watson@ucl.ac.uk

Abstract

Density estimation is a fundamental problem in statistics, and any attempt to do so in high dimensions typically requires strong assumptions or complex deep learning architectures. An important application for density estimators is synthetic data generation, an area currently dominated by neural networks that often demand enormous training datasets and extensive tuning. We propose a new method based on unsupervised random forests for estimating smooth densities in arbitrary dimensions without parametric constraints, as well as generating realistic synthetic data. We prove the consistency of our approach and demonstrate its advantages over existing tree-based density estimators, which generally rely on ill-chosen split criteria and do not scale well with data dimensionality. Experiments illustrate that our algorithm compares favorably to state-of-the-art deep learning generative models, achieving superior performance in a range of benchmark trials while executing about two orders of magnitude faster on average. Our method is implemented in easy-to-use R and Python packages.

1 Introduction

Density estimation is a fundamental unsupervised learning task, an essential subroutine in various methods for data imputation [28, 68], clustering [11, 67], anomaly detection [16, 59], and classification [48, 82]. One important application for density estimators is generative modeling, where we aim to create synthetic samples that mimic the characteristics of real data. These simulations can be used to test the robustness of classifiers [76, 15], augment training sets with synthetic samples [66, 47], or study complex systems without compromising the privacy of data subjects [4, 89].

The current state of the art in generative modeling relies on deep neural networks, which have proven remarkably adept at creating realistic images, audio, and even video data, as dramatically exemplified by the proliferation of so-called “deepfakes” [55]. Architectures built on variational autoencoders (VAEs) [42] and generative adversarial networks (GANs) [35] have dominated the field for the last decade. While these algorithms are highly effective with structured data such as images and text, they can struggle to produce good results on tabular data with mixed continuous and categorical covariates. Even when successful, VAEs and GANs are notoriously data-hungry and require extensive tuning.

We propose a fast, flexible method for smooth density estimation and generative modeling with unsupervised random forests. Our algorithm naturally accommodates mixed data in tabular settings, and performs well on small and large datasets using the computational resources of a standard laptop. It is more accurate than leading tree-based alternatives and about 100 times faster than deep learning solutions, with little or no tuning required.

Following a brief discussion of related work (Sect. 2), we review relevant notation and background on random forests (Sect. 3). We motivate our method with theoretical results that guarantee convergence under reasonable assumptions (Sect. 4), and illustrate its performance on a range of benchmark tasks (Sect. 5). We conclude with a discussion (Sect. 6) and directions for future work (Sect. 7).

2 Related Work

A random forest (RF) is a bootstrap-aggregated (bagged) ensemble of independently randomized trees [12], typically built using the greedy classification and regression tree (CART) algorithm [14]. RFs are extremely popular and effective, widely used in areas like bioinformatics [17], remote sensing [6], and ecology [21], as well as more generic prediction tasks [29]. Advantages include their efficiency (RFs are embarrassingly parallelizable), ease of use (they require minimal tuning), and ability to adapt to sparse signals (uninformative features are rarely selected for splits).

It is well-known that tree-based models can approximate joint distributions. Several authors advocate using leaf nodes of CART trees as piecewise constant density estimators [65, 86, 19]. While this method provably converges on the true density in the limit of infinite data, finite sample performance is inevitably rough and discontinuous. Smooth results can be obtained by applying either kernel density estimation (KDE) or maximum likelihood estimation (MLE) within each leaf [75, 37, 46, 65, 20, 19], a version of which we develop further below. Existing methods have mostly been limited to supervised trees rather than unsupervised forests, and are inefficient with more than a handful of covariates. Another strategy, better suited to high-dimensional data, uses Chow-Liu trees to learn a second-order approximation to the underlying joint distribution [5, 45, 64]. Whereas these methods estimate a series of bivariate densities over the full support of the data, we reduce complexity even further, computing univariate densities in smaller subregions.

The contemporary literature on generative models arguably begins with the introduction of VAEs [42] and GANs [35], which jointly optimize parameters for network pairs—encoder-decoder and generator-discriminator, respectively—via stochastic gradient descent. Variational generators are a special case of normalizing flows, a family of methods for mapping base distributions (e.g., standard normals) to observed distributions through a sequence of diffeomorphic transformations [60]. Various extensions of these approaches have been developed [39, 2], including some designed for mixed data in the tabular setting [18, 40, 87]. For an overview of deep generative modeling techniques, see [80]. Other approaches to density estimation and generative sampling include Bayesian networks [38, 43, 90] and copula methods [57, 56, 78].

Despite the popularity of tree-based density estimators, they are rarely if ever used for fully synthetic data generation. Instead, trees and forests are commonly used for *conditional* density estimation [77, 79, 19, 49]. We highlight that methods optimized for this task are often ill-suited to generative modeling, since their reliance on supervised signals limits their ability to capture dependencies between features with little predictive value for the selected outcome variable(s).

3 Background

Consider the binary classification setting with training data $\mathcal{D} = \{(\mathbf{x}_i, y_i)\}_{i=1}^n$, where $\mathbf{x}_i \in \mathcal{X} \subseteq \mathbb{R}^d$ and $y_i \in \mathcal{Y} = \{0, 1\}$. We assume that samples are independent and identically distributed (i.i.d.) according to some fixed but unknown distribution P with density p . The classic RF algorithm takes B bootstrap samples from \mathcal{D} and fits a binary decision tree for each, in which observations are recursively partitioned according to some optimization target (e.g., Gini index) evaluated on a random subset of features at each node. Resulting splits are of the form $\mathbb{I}[X_j > x]$ for some feature $X_j, j \in [d] = \{1, \dots, d\}$, and value $x \in \mathcal{X}_j$, where $\mathbb{I}[\cdot]$ represents the indicator function and data pass to left or right child nodes depending on whether they satisfy the inequality. Splits continue until some stopping criterion is met (e.g., purity). Terminal nodes, a.k.a. *leaves*, describe hyperrectangles in feature space with boundaries given by the learned splits. This partitions the data into disjoint cells, which collectively cover all of \mathcal{X} . Each leaf is associated with a label $\hat{y} \in [0, 1]$, representing either the frequency of positive outcomes (soft labels) or the majority class (hard labels) within that cell.

Each new datapoint \mathbf{x} falls into one leaf in each tree. Predictions are computed by aggregating over the trees, e.g. by tallying votes across all B basis functions of the ensemble. Let ϕ_b^ℓ denote the conjunction of inequalities that characterize membership in leaf $\ell \in [L_b]$, where L_b is the number of leaves in tree $b \in [B]$, with corresponding hyperrectangular subspace $\mathcal{X}_b^\ell \subset \mathcal{X}$. Let n_b be the number of training samples for tree b , and n_b^ℓ the number of samples that fall into leaf ℓ of b . The ratio n_b^ℓ/n_b represents an empirical estimate of the leaf’s coverage $p(\phi_b^\ell)$, i.e. the probability that a random \mathbf{x} falls within \mathcal{X}_b^ℓ .

Our method relies on the *unsupervised* random forest (URF) algorithm [72, 1, 51]. This procedure creates a synthetic dataset $\tilde{\mathbf{X}}$ of n observations by independently sampling from the marginals of \mathbf{X} , i.e. $\tilde{\mathbf{x}} \sim \prod_{j=1}^d P(X_j)$. An RF classifier is trained to distinguish between \mathbf{X} and $\tilde{\mathbf{X}}$, with labels indicating whether samples are original ($Y = 1$) or synthetic ($Y = 0$). We define empirical coverage for a URF

leaf to range over just the original data, $q(\phi_b^\ell) := \sum_{i: \mathbf{x}_i \in \mathcal{X}_b^\ell} y_i / (n_b/2)$, where the denominator reflects the requirement that trees be balanced w.r.t. Y . The method has expected accuracy $1/2$ in the worst case, corresponding to a dataset in which all features are mutually independent. However, if true accuracy converges to $1/2 + \epsilon$ for some $\epsilon > 0$, then consistent testing procedures will almost surely detect the discrepancy as n grows [41]. If this condition does not hold, then the generative modeling problem is trivial, since independent bootstraps or permutations of the original features are indistinguishable from \mathbf{X} .

4 Forests for Density Estimation and Generative Modeling

We introduce FORests for Density Estimation (FORDE) and FORests for GEnerative modeling (FORGE). Both algorithms are outlined in pseudocode below. Our basic strategy is to learn some function q that closely approximates the true density p , and use it to create new samples $\tilde{\mathbf{X}}$ that are indistinguishable in distribution from the original data \mathbf{X} .

Algorithm 1 FORDE

Input: Training dataset $\mathbf{X} \in \mathbb{R}^{n \times d}$
Output: Estimated density q

$f \leftarrow \text{UNSUPERVISED RRF}(\mathbf{X})$
for tree $b \in [B]$ **do**
 for leaf $\ell \in [L_b]$ **do**
 $\phi_b^\ell \leftarrow$ inequalities characterizing ℓ, b
 $q(\phi_b^\ell) \leftarrow \sum_{i: \mathbf{x}_i \in \mathcal{X}_b^\ell} y_i / (n_b/2)$
 for $j \in [d]$ **do**
 $\theta_{b,j}^\ell \leftarrow$ parameter(s) for $p(x_j | \phi_b^\ell)$
 $q(\cdot; \theta_{b,j}^\ell) \leftarrow$ corresponding pdf/pmf
 end for
 end for
end for

Algorithm 2 FORGE

Input: FORDE model q , target sample size m
Output: Synthetic dataset $\tilde{\mathbf{X}} \in \mathbb{R}^{m \times d}$

for $i \in [m]$ **do**
 Sample tree $b \in [B]$ uniformly
 Sample leaf $\ell \in [L_b]$ w.p. $q(\phi_b^\ell)$
 for $j \in [d]$ **do**
 Sample data $\tilde{x}_{ij} \sim q(\cdot; \theta_{b,j}^\ell)$
 end for
end for

The important point to recognize is that, if our URF has converged, then the features within each leaf will be jointly independent. This follows directly from the algorithm’s learning objective, which seeks to distinguish original from synthetic data in which all features are independent by construction. With sufficient sample size and tree depth, the algorithm continues splitting until no further dependencies can be exploited. This procedure makes local density estimation tractable, since we can simply run d separate univariate estimators within each leaf. This is exponentially easier than multivariate density estimation, which suffers from the notorious *curse of dimensionality*. Summarizing the challenges with estimating joint densities, one recent textbook on KDE concludes that “nonparametric methods for kernel density problems should not be used for high-dimensional data and it seems that a feasible dimensionality should not exceed five or six...” [36, p. 60]. By contrast, our method escapes the curse altogether by simplifying the density estimation task through well-chosen split criteria.

With our URF in hand, the algorithm proceeds as follows. For each tree b , we record the split criteria ϕ_b^ℓ and empirical coverage $q(\phi_b^\ell)$ of each leaf ℓ . Call these the *leaf parameters*. Then we estimate *distribution parameters* $\theta_{b,j}^\ell$ independently for each (original) X_j within \mathcal{X}_b^ℓ , e.g. the kernel bandwidth for KDE or class probabilities for MLE with categorical data. This completes Alg. 1. The generative model, Alg. 2, then follows a simple two-step procedure. First, sample a tree uniformly from $[B]$ and a leaf from that tree with probability $q(\phi_b^\ell)$. Next, sample data for each feature X_j according to the density/mass function parametrized by $\theta_{b,j}^\ell$. We repeat this procedure until the target number of synthetic samples has been generated.

We are deliberately agnostic about how distribution parameters $\theta_{b,j}^\ell$ should be learned, as this will tend to vary across features. In our theoretical analysis, we restrict our focus to continuous variables and consider a flexible family of KDE methods. For our experiments, we use MLE, assuming local normality for continuous data (effectively implementing a generalized Gaussian mixture model), and computing class probabilities for categorical variables. Both techniques work well in practice. We revisit this issue in Sect. 6.

Our estimated density takes the following form:

$$q(\mathbf{x}) = \frac{1}{B} \sum_{\ell, b: \mathbf{x} \in \mathcal{X}_b^\ell} q(\phi_b^\ell) \prod_{j=1}^d q(x_j; \theta_{b,j}^\ell). \quad (1)$$

Compare this with the true density, which can be written:

$$p(\mathbf{x}) = \frac{1}{B} \sum_{\ell, b: \mathbf{x} \in \mathcal{X}_b^\ell} p(\phi_b^\ell) p(\mathbf{x} | \phi_b^\ell). \quad (2)$$

In both cases, the density evaluated at a given point is just a coverage-weighted average of its density in all leaves whose split criteria it satisfies.

We show that $q(\mathbf{x})$ is a consistent estimator of $p(\mathbf{x})$. Following a common trend in the literature [7, 23, 71, 53, 83, 3, 61], we consider a slightly modified version of the RF algorithm for analysis. Specifically, we build trees using data subsamples rather than bootstraps and impose several further conditions specified below. Let $\eta(\mathbf{x}) := P(Y = 1 | \mathbf{x})$ be the true conditional probability function that we estimate via the URF f , with the second conditional moment $\eta_2(\mathbf{x}) := \mathbb{E}[Y^2 | \mathbf{x}]$. Predictions are made with the soft labeling approach described above. We make the following assumptions:

- (A1) The domain of \mathbf{X} is limited to the unit hypercube, $\mathcal{X} = [0, 1]^d$, and its density p is bounded away from 0 and ∞ .
- (A2) The conditional moments $\eta(\mathbf{x}), \eta_2(\mathbf{x})$ are Lipschitz-continuous. That is, there exist some constants $L_1, L_2 > 0$ such that, for all $\mathbf{x}, \mathbf{x}' \in \mathcal{X}$, we have $|\eta(\mathbf{x}) - \eta(\mathbf{x}')| \leq L_1 \|\mathbf{x} - \mathbf{x}'\|$ and $|\eta_2(\mathbf{x}) - \eta_2(\mathbf{x}')| \leq L_2 \|\mathbf{x} - \mathbf{x}'\|$.
- (A3) Conditional probabilities are bounded away from the extrema of the unit interval, i.e. for all $\mathbf{x} \in \mathcal{X}, 0 < \eta(\mathbf{x}) < 1$.
- (A4) Trees are honest and regular, as defined by Wager and Athey [83]. That is, (i) training data for each tree is split into two subsets: one to learn split parameters, and the other to assign leaf labels; (ii) every split puts some fraction $\gamma \leq 0.2$ of the available observations into each child node; (iii) at each internal node, the probability that the tree splits on any given X_j is bounded from below by some $\pi > 0$; (iv) the subsample size n_b satisfies $n_b \rightarrow \infty$ and $n_b \log(n)^d / n \rightarrow 0$; (v) the minimum within-leaf sample size satisfies $\min_{\ell, b} (n_b^\ell) \rightarrow \infty$.
- (A5) The true density function p is smooth. Specifically, its second derivative p'' is finite, continuous, square integrable, and ultimately monotone.

(A1) is simply for notational convenience, and can be replaced without loss of generality by bounding the domain of \mathbf{X} with arbitrary constants. (A2) is a common learning theoretic assumption widely used in the analysis of RFs [7, 52, 31]. (A3) is a sort of overlap condition that ensures strictly positive conditional variance [83]. The tree specification conditions of (A4) were originally introduced in the context of RF regression analysis [83, 3, 61]. For reasons explained in Appx. A, they are better suited to our purpose than alternative consistency conditions reported for RF classifiers. Finally, (A5) imposes common conditions for KDE consistency [74, 84, 36].

Because we are concerned with L_2 -consistency, our loss function is the mean integrated squared error (MISE)¹, defined as:

$$\text{MISE}(p, q) := \mathbb{E} \left[\int_{\mathcal{X}} (p(\mathbf{x}) - q(\mathbf{x}))^2 d\mathbf{x} \right].$$

Our method admits three potential sources of error, quantified by the following residuals:

$$\epsilon_1 := \epsilon_1(\ell, b) := p(\phi_b^\ell) - q(\phi_b^\ell) \quad (3)$$

$$\epsilon_2 := \epsilon_2(\ell, b, \mathbf{x}) := \prod_{j=1}^d p(x_j | \phi_b^\ell) - \prod_{j=1}^d q(x_j; \theta_{b,j}^\ell) \quad (4)$$

$$\epsilon_3 := \epsilon_3(\ell, b, \mathbf{x}) := p(\mathbf{x} | \phi_b^\ell) - \prod_{j=1}^d p(x_j | \phi_b^\ell) \quad (5)$$

¹Alternative loss functions may also be suitable, e.g. information theoretic measures like the Kullback-Leibler divergence or integral probability metrics such as the Wasserstein distance.

We refer to these as errors of *coverage*, *density*, and *convergence*, respectively. Observe that ϵ_1 is a random variable that depends on ℓ and b , while ϵ_2, ϵ_3 are random variables depending on ℓ, b and \mathbf{x} . We drop the dependencies for ease of notation. (See Appx. A for all proofs.)

Lemma 1. The error of our estimator satisfies the following bound:

$$\text{MISE}(p, q) \leq 2B^{-2} \mathbb{E} \left[\int_{\mathcal{X}} \alpha^2 + \beta^2 d\mathbf{x} \right],$$

where

$$\alpha := \sum_{\ell, b: \mathbf{x} \in \mathcal{X}_b^\ell} p(\phi_b^\ell) \epsilon_3 \quad \text{and} \quad \beta := \sum_{\ell, b: \mathbf{x} \in \mathcal{X}_b^\ell} \left(p(\phi_b^\ell) \epsilon_2 + \epsilon_1 \prod_{j=1}^d p(x_j | \phi_b^\ell) - \epsilon_1 \epsilon_2 \right).$$

This lemma establishes that total error is bounded by a quadratic function of $\epsilon_1, \epsilon_2, \epsilon_3$. Our main result states that all three error sources vanish in the limit.

Theorem 1 (Consistency). *Under assumptions (A1)-(A5), Alg. 1 is L_2 -consistent. That is, the following holds almost surely:*

$$\lim_{n \rightarrow \infty} \text{MISE}(p, q) = 0.$$

Our consistency proof is fundamentally unlike those of piecewise constant density estimators with CART trees [65, 86, 19], which essentially treat base learners as adaptive histograms and rely on tree-wise convergence when leaf volume goes to zero [24, 48]. Alternative methods that perform KDE or MLE within each leaf do not come with theoretical guarantees [75, 37, 46, 65, 20]. Such algorithms are typically designed for *conditional* density estimation, and therefore require some outcome variable(s). This means that dependencies between features with little predictive value may be ignored, since trees are unlikely to split on them during model training. In the rare case that authors use some form of unsupervised splits, they make no effort to factorize the distribution and are therefore subject to the curse of dimensionality [20, Ch. 5]. By contrast, our method exploits URFs to find regions of local independence, and univariate density estimation to compute marginals within each leaf. Though our consistency result comes at the cost of some extra assumptions, we argue that this is a fair price to pay for the improved performance in finite samples.

To understand the reasons for this improvement, consider that piecewise constant estimators treat all points as equiprobable within each leaf. With continuous features, this supposition can only be justified through asymptotic arguments about vanishing volume. Smooth alternatives avoid this particular shortcoming, but unless their split procedure optimizes for local independence, these methods must model potentially complex dependencies within each leaf. Rather than face the curse of dimensionality just once, they now face it $\sum_{b=1}^B L_b$ times, in each instance operating with a limited dataset of n_b^ℓ samples. Alternatives based on Chow-Liu trees share our goal of simplifying density estimation by ruling out higher order dependencies, but the resulting approximations may be poor since they span the full support of the data.

5 Experiments

In this section, we present results from a wide range of experiments conducted on simulated and real-world datasets. In all cases, we use the default parameters of 10 trees with a leaf size of 5. Code for reproducing all results and figures is available at https://github.com/bips-hb/generative_rf.

5.1 Simulation

FORGE recreates visual patterns. We begin with a simple proof of concept experiment, illustrating our method on a handful of low-dimensional datasets that allow for easy visual assessment. The **cassini**, **shapes**, **smiley**, and **twomoons** problems are all three-dimensional examples that combine two continuous covariates with a categorical class label. We simulate $n = 1000$ samples from each data generating process (see Fig. 1, top row) and estimate densities using FORGE. We proceed to FORGE a synthetic dataset of $n = 1000$ samples (Fig. 1, bottom row) and compare results. We find that the model consistently approximates its target distribution with high fidelity. Classes are clearly distinguished in all cases, and

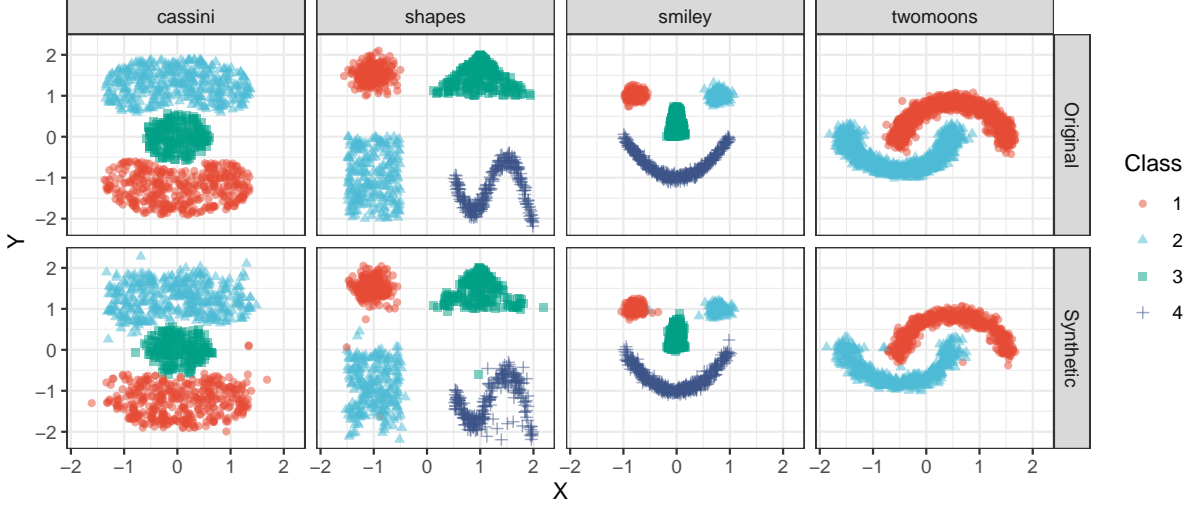


Figure 1: Visual examples. Original (top) and synthetic (bottom) data are presented for four three-dimensional problems with two continuous covariates and a single categorical feature.

the visual form of the original data is immediately recognizable. The fit is probably poorest on the sinusoidal curve of the **shapes** dataset, where the model has done a good job capturing the mean trend but apparently overestimated the variance. This can likely be mitigated with more trees and/or a larger training set.

FORGE outperforms alternative RF-based methods. We simulate data from a multivariate Gaussian distribution $\mathcal{N}(0, \Sigma)$, with Toeplitz covariance matrix $\Sigma_{ij} = 0.5^{|i-j|}$ and fixed $d = 10$. To compare against supervised methods, we also simulate a binary target $Y \sim \text{Bern}([1 + \exp(-\mathbf{X}\beta)]^{-1})$, where the coefficient vector β contains a varying proportion of 0’s (non-informative features) and 1’s (informative features). Parameters $\hat{\mu}$ and $\hat{\Sigma}$ are estimated from synthetic data via MLE. We record the Kullback–Leibler (KL) divergence² between the ground truth distribution $\mathcal{N}(0, \Sigma)$ and the estimated $\mathcal{N}(\hat{\mu}, \hat{\Sigma})$. We compare our method to piecewise constant (PWC) estimators with supervised and unsupervised split criteria,³ as well as generative forests (GeFs), a smooth conditional density estimation procedure [19].

Fig. 2 shows the average KL-divergence over 20 replicates for varying sample sizes (A) and levels of sparsity (B). For the former, we fix the proportion of informative features at 0.5; for the latter, we fix $n = 10,000$. We find that unsupervised methods dominate at all sample sizes, with the PWC variant performing well for small n before FORGE overtakes around $n = 1000$. We observe several interesting trends in the sparsity experiment, where PWC estimators appear to do worse with more informative features, while GeFs do best with very weak or very strong signals. This can be explained by the fact that splits are purely random when no features are informative, a strategy that is known to work well in noisy settings [34, 33]. Performance degrades as more informative features are added, since supervised models narrowly focus on these predictors to the exclusion of uninformative covariates, which comprise the majority of the data. Things reach a tipping point around 0.5, at which point most features provide signal and models gradually stabilize (PWC) or improve again (GeFs). Unsupervised split criteria, by contrast, show less variation in general and uniformly stronger performance in the case of FORGE.

5.2 Real Data

To evaluate the performance of FORGE on real-world datasets, we recreate a benchmarking pipeline originally proposed by Xu et al. [87]. They introduce the conditional tabular GAN (CTGAN) and tabular VAE (TVAE), two deep learning algorithms for generative modeling with mixed continuous and categorical features. It is straightforward to augment their benchmark with FORGED data to ensure adequate parameter configurations for deep learning competitors, and mitigate potential biases stemming from selective experimental designs.

²Note that the KL-divergence and the MISE are both nonnegative loss functions that equal 0 if and only if true and estimated densities are equivalent for all $\mathbf{x} \in \mathcal{X}$.

³Supervised PWC is simply an ensemble version of the classic method [37, 65, 86]. To the best of our knowledge, no one has previously proposed unsupervised PWC density estimation with CART trees. This can be understood as a variant of our approach in which all marginals are uniform within each leaf.

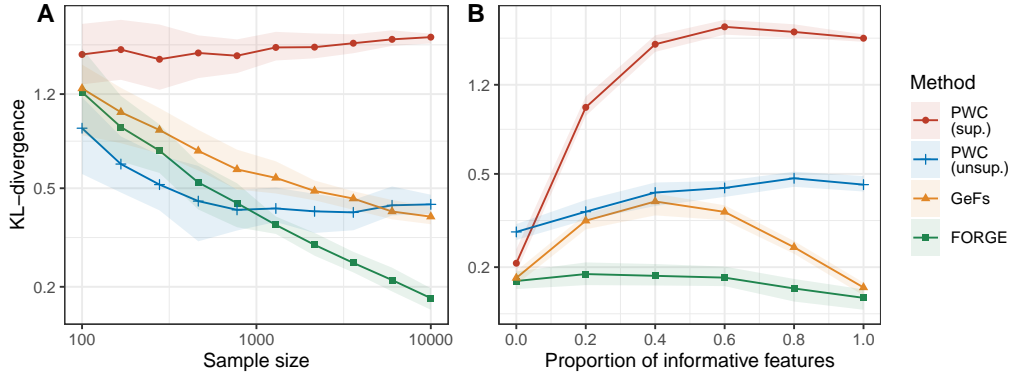


Figure 2: KL-divergence between ground truth and estimated distribution of data generated with PWC (supervised and unsupervised), GeFs, and FORGE for varying sample size (A) and sparsity (B).

A complete summary of the experimental setup is presented in Appx. B. Briefly, we take seven benchmark datasets for classification and partition the samples into training and test sets, which we denote by $\mathbf{Z}_{\text{trn}} = (\mathbf{X}_{\text{trn}}, Y_{\text{trn}})$ and $\mathbf{Z}_{\text{tst}} = (\mathbf{X}_{\text{tst}}, Y_{\text{tst}})$, respectively. \mathbf{Z}_{trn} is then used as input to a series of generative models, each of which creates a synthetic training set $\tilde{\mathbf{Z}}_{\text{trn}}$ of the same sample size as the original. Several classifiers are then trained on $\tilde{\mathbf{Z}}_{\text{trn}}$ and evaluated on \mathbf{Z}_{tst} , with performance metrics averaged across learners. Results are benchmarked against the same set of algorithms, now trained on the original data \mathbf{Z}_{trn} . We refer to this model as the *Oracle*, since it should perform no worse in expectation than any classifier trained on synthetic data. However, if the generative model has done a good job learning the true joint density, then differences between the Oracle and its competitors may be negligible. Similar approaches are widely used in the evaluation of GANs [88, 73, 69]; for a critical discussion, see [66].

Results are reported in Table 1, where we average over five trials of data synthesis and subsequent supervised learning. Performance is evaluated via accuracy and F1-score, as well as wall time. We find that FORGE is the most accurate method in five out of seven tasks, and has the highest F1-score in six out of seven. More impressive, it executes over 100 times faster than CTGAN and over 50 times faster than TVAE on average. Differences in compute time would be even more dramatic if these deep learning algorithms were configured with a CPU backend (we used GPUs here), or if FORGE were run using more extensive parallelization (we distribute the job across 10 cores). This comparison also obscures the extra time required to tune hyperparameters for these complex models, whereas our method is an off-the-shelf solution that works well with default settings.

5.3 Run Time

To further demonstrate the computational efficiency of FORGE relative to deep learning methods, we conduct a run time experiment using the smallest dataset above, **adult**. By repeatedly sampling stratified subsets—varying both sample size n and dimensionality d —and measuring the time needed to generate synthetic samples, we illustrate how complexity scales with n and d (see Fig. 3 for a comparison in terms of wall time and Appx. B for results in terms of process time). For this experiment, we ran CTGAN and TVAE with both CPU and GPU backends. We use default parameters for both algorithms, which include automated parallelization over all available cores (24 in this experiment). The results are stark. For those with limited access to GPUs, deep learning methods may be completely infeasible for large datasets. Even when GPUs are available, FORGE scales far better, executing about 35 times faster than TVAE and 85 times faster than CTGAN in this example. Note that FORGE also outperforms both in terms of accuracy and F1-score for the **adult** dataset, so the speedup need not come at the cost of performance.

6 Discussion

By analogy with the GAN approach, our URF f can be understood as a “discriminator”, distinguishing original samples from (naïvely constructed) synthetic data. We considered iterative procedures inspired by GANs, in which a new RF classifier f' is trained to discriminate original samples from FORGE outputs. The resulting synthetic data would then be used to train another RF f'' , and so on until discriminators

Table 1: Average results across five replicates. We report regular F1-scores for binary classification tasks, and F1 macro-scores for multiclass problems (see Appx. B for details). The dimensionality d reported amongst other dataset characteristics excludes the target variable. Wall time is measured with GPU backends for CTGAN and TVAE, while FORGE is run in parallel on 10 CPU cores.

Dataset	Characteristics	Model	Accuracy (sd)	F1 (sd)	Time in sec
adult		<i>Oracle</i>	<i>0.828 (0.006)</i>	<i>0.884 (0.004)</i>	
	$n = 32,561$	FORGE	0.819 (0.006)	0.877 (0.005)	2.9
	$d = 14$	CTGAN	0.786 (0.020)	0.853 (0.019)	263.3
	classes = 2	TVAE	0.804 (0.007)	0.865 (0.006)	115.1
census		<i>Oracle</i>	<i>0.922 (0.002)</i>	<i>0.957 (0.001)</i>	
	$n = 298,006$	FORGE	0.903 (0.019)	0.946 (0.012)	53.2
	$d = 40$	CTGAN	0.916 (0.015)	0.954 (0.009)	4,287.8
	classes = 2	TVAE	0.928 (0.007)	0.961 (0.004)	1,814.9
coverttype		<i>Oracle</i>	<i>0.895 (0.000)</i>	<i>0.838 (0.000)</i>	
	$n = 581,012$	FORGE	0.707 (0.006)	0.549 (0.006)	103.5
	$d = 54$	CTGAN	0.633 (0.009)	0.400 (0.009)	13,387.2
	classes = 7	TVAE	0.698 (0.013)	0.459 (0.013)	4,882.0
credit		<i>Oracle</i>	<i>0.997 (0.001)</i>	<i>0.607 (0.029)</i>	
	$n = 284,807$	FORGE	0.995 (0.001)	0.527 (0.036)	32.2
	$d = 30$	CTGAN	0.881 (0.099)	0.047 (0.031)	4,898.0
	classes = 2	TVAE	0.998 (0.000)	0.000 (0.000)	3,847.6
intrusion		<i>Oracle</i>	<i>0.998 (0.001)</i>	<i>0.833 (0.001)</i>	
	$n = 494,021$	FORGE	0.993 (0.001)	0.656 (0.001)	68.2
	$d = 40$	CTGAN	0.944 (0.088)	0.645 (0.088)	8,749.3
	classes = 5	TVAE	0.990 (0.002)	0.598 (0.002)	4,306.0
mnist12		<i>Oracle</i>	<i>0.892 (0.003)</i>	<i>0.891 (0.003)</i>	
	$n = 70,000$	FORGE	0.799 (0.007)	0.795 (0.007)	32.5
	$d = 144$	CTGAN	0.172 (0.032)	0.138 (0.032)	2,737.4
	classes = 10	TVAE	0.763 (0.002)	0.761 (0.002)	1,143.8
mnist28		<i>Oracle</i>	<i>0.918 (0.002)</i>	<i>0.917 (0.002)</i>	
	$n = 70,000$	FORGE	0.729 (0.008)	0.723 (0.008)	169.5
	$d = 784$	CTGAN	0.197 (0.051)	0.167 (0.051)	14,415.4
	classes = 10	TVAE	0.698 (0.016)	0.697 (0.016)	5,056.0

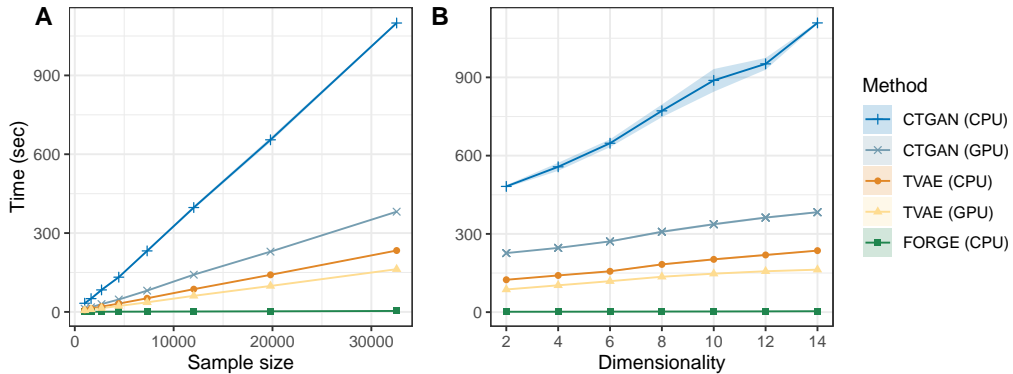


Figure 3: Complexity curves. (A): Wall time as a function of sample size, using stratified subsamples of the **adult** dataset. (B): Wall time as a function of dimensionality, using random features from the **adult** dataset.

cannot improve any further. The problem with this method is that features will not in general be jointly independent within the leaves of a classifier trained to distinguish between original and FORGED samples, unlike in the URF we use. Since this property justifies the univariate density estimation subroutine, the iterative approach cannot be applied here. However, for complex problems with structured data, iterative variants of our method may warrant further investigation.

One potential difficulty for our method is selecting an optimal density estimation procedure. KDE relies on a smoothness assumption (A5), while MLE requires a (local) parametric model. Both methods will struggle when their assumptions are violated. Resampling alternatives such as permutations or bootstrapping do not produce any data that was not observed in the training set and may therefore raise privacy concerns. No method is generally guaranteed to strike the optimal balance between efficiency, accuracy, and privacy, and so the choice of which estimation procedure to employ for specific variables is irreducibly context-dependent.

We emphasize that FORDE performs well in a range of settings without any model tuning. However, we acknowledge that optimal performance likely depends on URF parameters [70, 63]. In particular, there is an inherent trade-off between the goals of minimizing errors of density (ϵ_2) and errors of convergence (ϵ_3) in finite samples. Grow trees too deep, and leaves will not contain enough data to accurately estimate marginal densities; grow trees too shallow, and the URF will fail to converge, resulting in violations of local independence. Meanwhile, the *mtry* parameter, which controls how many features are sampled for potential splits at each internal node, has been shown to control sparsity in low signal-to-noise regimes [54]. Smaller values of *mtry* may therefore be appropriate when ϵ_3 is large, in order to regularize the URF. Adding more trees can stabilize results, though this incurs extra computational cost in both time and memory [62]. Despite these considerations, we reiterate that RFs are known to do well with default parameters, a trait that FORDE appears to inherit, judging by our experiments. We leave the task of rigorously exploring the impact of URF parameters to future work.

The ethical implications of generative models are potentially fraught. Deepfakes have attracted particular attention in this regard [25, 58, 22], as they can deceive their audience into believing that people said or did things they never in fact said or did. These dangers are most acute with convolutional neural networks or other architectures optimized for visual and audio data. Despite and in full awareness of these concerns, we highlight an ethical opportunity presented by FORGE, which can preserve the privacy of data subjects by creating datasets that capture all relevant signals without exposing the personal information of any individual. This is especially valuable in sensitive areas like healthcare and finance, where data breaches are fairly common and potentially disastrous. As with all powerful technologies, caution is advised and regulatory frameworks are welcome.

7 Conclusion

We have introduced a novel procedure for learning joint densities and generating synthetic data using unsupervised random forests. The method is provably consistent under reasonable assumptions, and performs well in experiments on simulated and real-world examples. Our FORDE algorithm is more accurate than leading tree-based alternatives, and more scalable than methods that require multivariate density estimation. Our FORGE algorithm is competitive with state-of-the-art deep learning models for data generation, and routinely executes some 100 times faster.

Future work will explore further applications for these methods, such as outlier detection, clustering, and classification, as well as potential connections with differential privacy [27]. Alternative tree-based solutions based on gradient boosting also warrant further exploration, especially given some promising recent developments in this area [30, 32].

Acknowledgments

DSW was funded by ONR grant 62909-19-1-2096. MNW was funded by the German Research Foundation (DFG) – Emmy Noether Grant 437611051 and by the U Bremen Research Alliance.

References

- [1] Nelson Lee Afanador, Agnieszka Smolinska, Thanh N. Tran, and Lionel Blanchet. Unsupervised random forest: a tutorial with case studies. *J. Chemom.*, 30(5):232–241, 2016.
- [2] Martin Arjovsky, Soumith Chintala, and Léon Bottou. Wasserstein generative adversarial networks. In *Proceedings of the 34th International Conference on Machine Learning*, page 214–223, 2017.
- [3] Susan Athey, Julie Tibshirani, and Stefan Wager. Generalized random forests. *Ann. Statist.*, 47(2): 1148–1178, 2019.
- [4] Sean Augenstein, H. Brendan McMahan, Daniel Ramage, Swaroop Ramaswamy, Peter Kairouz, Mingqing Chen, Rajiv Mathews, and Blaise Agüera y Arcas. Generative models for effective ML on private, decentralized datasets. In *International Conference on Learning Representations*, 2020.
- [5] Francis R. Bach and Michael I. Jordan. Beyond independent components: Trees and clusters. *J. Mach. Learn. Res.*, 4:1205–1233, 2003.
- [6] Mariana Belgiu and Lucian Drăguț. Random forest in remote sensing: A review of applications and future directions. *ISPRS J. Photogramm. Remote Sens.*, 114:24–31, 2016.
- [7] Gérard Biau. Analysis of a random forests model. *J. Mach. Learn. Res.*, 13:1063–1095, 2012.
- [8] Gérard Biau, Luc Devroye, and Gábor Lugosi. Consistency of random forests and other averaging classifiers. *J. Mach. Learn. Res.*, 9(66):2015–2033, 2008.
- [9] Gérard Biau and Luc Devroye. On the layered nearest neighbour estimate, the bagged nearest neighbour estimate and the random forest method in regression and classification. *J. Multivar. Anal.*, 101(10):2499–2518, 2010.
- [10] Jock A. Blackard. Coverttype data set, 1999. URL <https://archive.ics.uci.edu/ml/datasets/coverttype>.
- [11] Max Bramer. *Clustering*, pages 221–238. Springer, London, UK, 2007.
- [12] Leo Breiman. Random forests. *Mach. Learn.*, 45(1):1–33, 2001.
- [13] Leo Breiman. Consistency for a simple model of random forests. Technical Report 670, Statistics Department, UC Berkeley, Berkeley, CA, 2004.
- [14] Leo Breiman, Jerome Friedman, C. J. Stone, and R. A. Olshen. *Classification and Regression Trees*. Taylor & Francis, Boca Raton, FL, 1984.
- [15] Igor Buzhinsky, Arseny Nerinovsky, and Stavros Tripakis. Metrics and methods for robustness evaluation of neural networks with generative models. *Mach. Learn.*, 2021.
- [16] Varun Chandola, Arindam Banerjee, and Vipin Kumar. Anomaly detection: A survey. *ACM Comput. Surv.*, 41(3), 2009.
- [17] Xi Chen and Hemant Ishwaran. Random forests for genomic data analysis. *Genomics*, 99(6):323–329, 2012.
- [18] Edward Choi, Siddharth Biswal, Bradley Malin, Jon Duke, Walter F. Stewart, and Jimeng Sun. Generating multi-label discrete patient records using generative adversarial networks. In *Proceedings of the 2nd Machine Learning for Healthcare Conference*, volume 68 of *Proceedings of Machine Learning Research*, pages 286–305, 2017.
- [19] Alvaro Correia, Robert Peharz, and Cassio P de Campos. Joints in random forests. In *Advances in Neural Information Processing Systems*, volume 33, pages 11404–11415, 2020.
- [20] Antonio Criminisi, Jamie Shotton, and Ender Konukoglu. *Decision Forests: A Unified Framework for Classification, Regression, Density Estimation, Manifold Learning and Semi-Supervised Learning*, volume 7, pages 81–227. NOW Publishers, Norwell, MA, 2012.

- [21] D. Richard Cutler, Thomas C. Edwards Jr., Karen H. Beard, Adele Cutler, Kyle T. Hess, Jacob Gibson, and Joshua J. Lawler. Random forests for classification in ecology. *Ecology*, 88(11):2783–2792, 2007.
- [22] Adrienne de Ruiter. The distinct wrong of deepfakes. *Philos. Technol.*, 34(4):1311–1332, 2021.
- [23] Misha Denil, David Matheson, and Nando De Freitas. Narrowing the gap: Random forests in theory and in practice. In *Proceedings of the 31st International Conference on Machine Learning*, pages 665–673, 2014.
- [24] Luc Devroye, László Györfi, and Gábor Lugosi. *A Probabilistic Theory of Pattern Recognition*. Springer-Verlag, New York, 1996.
- [25] Nicholas Diakopoulos and Deborah Johnson. Anticipating and addressing the ethical implications of deepfakes in the context of elections. *New Media & Society*, 23(7):2072–2098, 2021.
- [26] Dheeru Dua and Casey Graff. UCI machine learning repository, 2019. URL <http://archive.ics.uci.edu/ml>.
- [27] Cynthia Dwork. Differential privacy: A survey of results. In *Theory and Applications of Models of Computation*, volume 4978, pages 1–19, Berlin, Heidelberg, 2008. Springer.
- [28] Bradley Efron. Missing data, imputation, and the bootstrap. *J. Am. Stat. Assoc.*, 89(426):463–475, 1994.
- [29] Manuel Fernández-Delgado, Eva Cernadas, Senén Barro, and Dinani Amorim. Do we need hundreds of classifiers to solve real world classification problems? *J. Mach. Learn. Res.*, 15(90):3133–3181, 2014.
- [30] Jerome H. Friedman. Contrast trees and distribution boosting. *Proc. Natl. Acad. Sci.*, 117(35):21175–21184, 2020.
- [31] Wei Gao and Zhi-Hua Zhou. Towards convergence rate analysis of random forests for classification. In *Advances in Neural Information Processing Systems*, volume 33, pages 9300–9311, 2020.
- [32] Zijun Gao and Trevor Hastie. LinCDE: Conditional density estimation via Lindsey’s method. *J. Mach. Learn. Res.*, 23(52):1–55, 2022.
- [33] Robin Genuer. Variance reduction in purely random forests. *J. Nonparametr. Stat.*, 24(3):543–562, 2012.
- [34] Pierre Geurts, Damien Ernst, and Louis Wehenkel. Extremely randomized trees. *Mach. Learn.*, 63(1):3–42, 2006.
- [35] Ian J. Goodfellow, Jean Pouget-Abadie, Mehdi Mirza, Bing Xu, David Warde-Farley, Sherjil Ozair, Aaron Courville, and Yoshua Bengio. Generative adversarial nets. In *Advances in Neural Information Processing Systems*, volume 27, page 2672–2680, 2014.
- [36] Artur Gramacki. *Nonparametric Kernel Density Estimation and Its Computational Aspects*. Springer, Cham, 2018.
- [37] Alexander G. Gray and Andrew W. Moore. Nonparametric density estimation: Toward computational tractability. In *Proceedings of the 2003 SIAM International Conference on Data Mining (SDM)*, pages 203–211, 2003.
- [38] David Heckerman, Dan Geiger, and David M Chickering. Learning Bayesian networks: The combination of knowledge and statistical data. *Mach. Learn.*, 20(3):197–243, 1995.
- [39] Irina Higgins, Loïc Matthey, Arka Pal, Christopher Burgess, Xavier Glorot, Matthew Botvinick, Shakir Mohamed, and Alexander Lerchner. β -VAE: Learning basic visual concepts with a constrained variational framework. In *International Conference on Learning Representations*, 2017.
- [40] James Jordon, Jinsung Yoon, and Mihaela van der Schaar. PATE-GAN: generating synthetic data with differential privacy guarantees. In *International Conference on Learning Representations*, 2019.

- [41] Ilmun Kim, Aaditya Ramdas, Aarti Singh, and Larry Wasserman. Classification accuracy as a proxy for two-sample testing. *Ann. Stat.*, 49(1):411 – 434, 2021.
- [42] Diederik Kingma and Max Welling. Auto-encoding variational Bayes. In *International Conference on Learning Representations*, 2013.
- [43] Steffen L Lauritzen. *Graphical Models*. Oxford Statistical Science Series. Clarendon Press, Oxford, 1996.
- [44] Yann LeCun, Léon Bottou, Yoshua Bengio, and Patrick Haffner. Gradient-based learning applied to document recognition. *Proceedings of the IEEE*, 86(11):2278–2324, 1998.
- [45] Han Liu, Min Xu, Haijie Gu, Anupam Gupta, John Lafferty, and Larry Wasserman. Forest density estimation. *J. Mach. Learn. Res.*, 12(25):907–951, 2011.
- [46] Wei-Yin Loh. Improving the precision of classification trees. *Ann. Appl. Stat.*, 3(4):1710 – 1737, 2009.
- [47] Romain Lopez, Jeffrey Regier, Michael B Cole, Michael I Jordan, and Nir Yosef. Deep generative modeling for single-cell transcriptomics. *Nat. Methods*, 15(12):1053–1058, 2018. ISSN 1548-7105.
- [48] Gábor Lugosi and Andrew Nobel. Consistency of data-driven histogram methods for density estimation and classification. *Ann. Stat.*, 24(2):687 – 706, 1996.
- [49] Scott M Lundberg, Gabriel Erion, Hugh Chen, Alex DeGrave, Jordan M Prutkin, Bala Nair, Ronit Katz, Jonathan Himmelfarb, Nisha Bansal, and Su-In Lee. From local explanations to global understanding with explainable AI for trees. *Nat. Mach. Intell.*, 2(1):56–67, 2020.
- [50] J.D. Malley, J. Kruppa, A. Dasgupta, K.G. Malley, and A. Ziegler. Probability Machines: Consistent probability estimation using nonparametric learning machines. *Methods Inf. Med.*, 51(1):74–81, 2012.
- [51] Alejandro Mantero and Hemant Ishwaran. Unsupervised random forests. *Stat. Anal. Data. Min.*, 14(2):144–167, 2021.
- [52] Nicolai Meinshausen. Quantile regression forests. *J. Mach. Learn. Res.*, 7:983–999, 2006.
- [53] Lucas Mentch and Giles Hooker. Quantifying uncertainty in random forests via confidence intervals and hypothesis tests. *J. Mach. Learn. Res.*, 17(26), 2016.
- [54] Lucas Mentch and Siyu Zhou. Randomization as regularization: A degrees of freedom explanation for random forest success. *J Mach. Learn. Res.*, 21(171), 2020.
- [55] Yisroel Mirsky and Wenke Lee. The creation and detection of deepfakes: A survey. *ACM Comput. Surv.*, 54(1), 2021.
- [56] Thomas Nagler and Claudia Czado. Evading the curse of dimensionality in nonparametric density estimation with simplified vine copulas. *J. Multivar. Anal.*, 151:69–89, 2016.
- [57] Roger B Nelsen. *An Introduction to Copulas*. Lecture notes in statistics. Springer, New York, 1999.
- [58] Carl Öhman. Introducing the pervert’s dilemma: a contribution to the critique of deepfake pornography. *Ethics Inf. Technol.*, 22(2):133–140, 2020.
- [59] Guansong Pang, Chunhua Shen, Longbing Cao, and Anton Van Den Hengel. Deep learning for anomaly detection: A review. *ACM Comput. Surv.*, 54(2), 2021.
- [60] George Papamakarios, Eric Nalisnick, Danilo Jimenez Rezende, Shakir Mohamed, and Balaji Lakshminarayanan. Normalizing flows for probabilistic modeling and inference. *J. Mach. Learn. Res.*, 22(57):1–64, 2021.
- [61] Wei Peng, Tim Coleman, and Lucas Mentch. Rates of convergence for random forests via generalized U-statistics. *Electron. J. Stat.*, 16(1):232 – 292, 2022.
- [62] Philipp Probst and Anne-Laure Boulesteix. To tune or not to tune the number of trees in random forest. *J. Mach. Learn. Res.*, 18(1):6673–6690, 2017.

- [63] Philipp Probst, Marvin N. Wright, and Anne-Laure Boulesteix. Hyperparameters and tuning strategies for random forest. *WIREs Data Mining and Knowledge Discovery*, 9(3):e1301, 2019.
- [64] Tahrima Rahman, Prasanna Kothalkar, and Vibhav Gogate. Cutset networks: A simple, tractable, and scalable approach for improving the accuracy of Chow-Liu trees. In *Machine Learning and Knowledge Discovery in Databases*, pages 630–645, Berlin, Heidelberg, 2014. Springer Berlin Heidelberg.
- [65] Parikshit Ram and Alexander G. Gray. Density estimation trees. In *Proceedings of the 17th ACM SIGKDD International Conference on Knowledge Discovery and Data Mining*, page 627–635, 2011.
- [66] Suman Ravuri and Oriol Vinyals. Classification accuracy score for conditional generative models. In *Advances in Neural Information Processing Systems*, volume 32, 2019.
- [67] Lior Rokach and Oded Maimon. *Clustering Methods*, pages 321–352. Springer US, Boston, MA, 2005.
- [68] Donald B. Rubin. Multiple imputation after 18+ years. *J. Am. Stat. Assoc.*, 91(434):473–489, 1996.
- [69] Shibani Santurkar, Ludwig Schmidt, and Aleksander Madry. A classification-based study of covariate shift in GAN distributions. In *Proceedings of the 35th International Conference on Machine Learning*, volume 80, pages 4480–4489, 2018.
- [70] Erwan Scornet. Tuning parameters in random forests. *ESAIM: Procs*, 60:144–162, 2017.
- [71] Erwan Scornet, Gerard Biau, and Jean Philippe Vert. Consistency of random forests. *Ann. Statist.*, 43(4):1716–1741, 2015.
- [72] Tao Shi and Steve Horvath. Unsupervised learning with random forest predictors. *J. Comput. Graph. Stat.*, 15(1):118–138, 2006.
- [73] Konstantin Shmelkov, Cordelia Schmid, and Karteek Alahari. How good is my GAN? In *Computer Vision – ECCV 2018*, pages 218–234, Cham, 2018. Springer International Publishing.
- [74] Bernard Silverman. *Density Estimation for Statistics and Data Analysis*. Chapman & Hall, London, 1986.
- [75] Padhraic Smyth, Alexander G. Gray, and Usama M. Fayyad. Retrofitting decision tree classifiers using kernel density estimation. In *Proceedings of the 12th International Conference on International Conference on Machine Learning*, page 506–514, 1995.
- [76] Yang Song, Rui Shu, Nate Kushman, and Stefano Ermon. Constructing unrestricted adversarial examples with generative models. In *Advances in Neural Information Processing Systems*, volume 31, 2018.
- [77] Daniel J Stekhoven and Peter Bühlmann. MissForest—non-parametric missing value imputation for mixed-type data. *Bioinformatics*, 28(1):112–118, 2011.
- [78] Yi Sun, Alfredo Cuesta-Infante, and Kalyan Veeramachaneni. Learning vine copula models for synthetic data generation. In *Proceedings of the 33rd AAAI Conference*, pages 5049–5057, 2019.
- [79] Fei Tang and Hemant Ishwaran. Random forest missing data algorithms. *Stat. Anal. Data Min.*, 10(6):363–377, 2017.
- [80] Jakub Tomczak. *Deep Generative Models*. Springer, New York, 2022.
- [81] V. N. Vapnik and A. Ya. Chervonenkis. *On the Uniform Convergence of Relative Frequencies of Events to Their Probabilities*, pages 11–30. Springer International Publishing, Cham, 2015.
- [82] Pascal Vincent and Yoshua Bengio. Manifold Parzen windows. In *Advances in Neural Information Processing Systems*, volume 15, 2002.
- [83] Stefan Wager and Susan Athey. Estimation and inference of heterogeneous treatment effects using random forests. *J. Am. Stat. Assoc.*, 113(523):1228–1242, 2018.
- [84] M.P. Wand and M.C. Jones. *Kernel Smoothing*. Chapman & Hall, Boca Raton, FL, 1994.

- [85] Worldline and the Machine Learning Group of ULB (Université Libre de Bruxelles). Credit card fraud detection data. license: Open database., 2013. URL <https://www.kaggle.com/datasets/mlg-ulb/creditcardfraud>.
- [86] Ke Wu, Kun Zhang, Wei Fan, Andrea Edwards, and Philip S. Yu. RS-Forest: A rapid density estimator for streaming anomaly detection. In *2014 IEEE International Conference on Data Mining*, pages 600–609, 2014.
- [87] Lei Xu, Maria Skoularidou, Alfredo Cuesta-Infante, and Kalyan Veeramachaneni. Modeling tabular data using conditional GAN. In *Advances in Neural Information Processing Systems*, volume 32, 2019.
- [88] Jianwei Yang, Anitha Kannan, Dhruv Batra, and Devi Parikh. LR-GAN: Layered recursive generative adversarial networks for image generation. In *International Conference on Learning Representations*, 2017.
- [89] Burak Yelmen, Aurélien Decelle, Linda Ongaro, Davide Marnetto, Corentin Tallec, Francesco Montinaro, Cyril Furtlehner, Luca Pagani, and Flora Jay. Creating artificial human genomes using generative neural networks. *PLOS Genetics*, 17(2):1–22, 02 2021.
- [90] Jun Zhang, Graham Cormode, Cecilia M. Procopiuc, Divesh Srivastava, and Xiaokui Xiao. Privbayes: Private data release via Bayesian networks. *ACM Trans. Database Syst.*, 42(4), 2017.

A Proofs

A.1 Proof of Lemma 1

Define the first-order approximation to p satisfying local independence:

$$\hat{p}(\mathbf{x}) = \frac{1}{B} \sum_{\ell, b: \mathbf{x} \in \mathcal{X}_b^\ell} p(\phi_b^\ell) \prod_{j=1}^d p(x_j | \phi_b^\ell).$$

We also define the root integrated squared error (RISE), i.e. the Euclidean distance between probability densities:

$$\text{RISE}(p, q) := \left(\int_{\mathcal{X}} \left(p(\mathbf{x}) - q(\mathbf{x}) \right)^2 d\mathbf{x} \right)^{1/2}.$$

By the triangle inequality, we have:

$$\text{RISE}(p, q) \leq \text{RISE}(p, \hat{p}) + \text{RISE}(\hat{p}, q).$$

Squaring both sides, we get:

$$\text{ISE}(p, q) \leq \text{ISE}(p, \hat{p}) + \text{ISE}(\hat{p}, q) + 2 \text{RISE}(p, \hat{p}) \text{RISE}(\hat{p}, q).$$

Adding a nonnegative constant to the rhs, we can reduce the expression:

$$\begin{aligned} \text{ISE}(p, q) &\leq \text{ISE}(p, \hat{p}) + \text{ISE}(\hat{p}, q) + 2 \text{RISE}(p, \hat{p}) \text{RISE}(\hat{p}, q) + \left(\text{RISE}(p, \hat{p}) - \text{RISE}(\hat{p}, q) \right)^2 \\ &= 2 \left(\text{ISE}(p, \hat{p}) + \text{ISE}(\hat{p}, q) \right). \end{aligned}$$

Now observe that we can rewrite both ISE formulae in terms of our predefined residuals (Eqs. 3-5):

$$\begin{aligned} \text{ISE}(p, \hat{p}) &= \int_{\mathcal{X}} \left(\frac{1}{B} \sum_{\ell, b: \mathbf{x} \in \mathcal{X}_b^\ell} \left(p(\phi_b^\ell) p(\mathbf{x} | \phi_b^\ell) - p(\phi_b^\ell) \prod_{j=1}^d p(x_j | \phi_b^\ell) \right) \right)^2 d\mathbf{x} \\ &= \frac{1}{B^2} \int_{\mathcal{X}} \left(\sum_{\ell, b: \mathbf{x} \in \mathcal{X}_b^\ell} p(\phi_b^\ell) \epsilon_3 \right)^2 d\mathbf{x}. \\ \text{ISE}(\hat{p}, q) &= \int_{\mathcal{X}} \left(\frac{1}{B} \sum_{\ell, b: \mathbf{x} \in \mathcal{X}_b^\ell} \left(p(\phi_b^\ell) \prod_{j=1}^d p(x_j | \phi_b^\ell) - q(\phi_b^\ell) \prod_{j=1}^d q(x_j; \boldsymbol{\theta}_{b,j}^\ell) \right) \right)^2 d\mathbf{x} \\ &= \frac{1}{B^2} \int_{\mathcal{X}} \left(\sum_{\ell, b: \mathbf{x} \in \mathcal{X}_b^\ell} \left(p(\phi_b^\ell) \epsilon_2 + \epsilon_1 \prod_{j=1}^d p(x_j | \phi_b^\ell) - \epsilon_1 \epsilon_2 \right) \right)^2 d\mathbf{x}. \end{aligned}$$

We replace the interior squared terms for ease of presentation:

$$\begin{aligned} \alpha &:= \sum_{\ell, b: \mathbf{x} \in \mathcal{X}_b^\ell} p(\phi_b^\ell) \epsilon_3 \\ \beta &:= \sum_{\ell, b: \mathbf{x} \in \mathcal{X}_b^\ell} \left(p(\phi_b^\ell) \epsilon_2 + \epsilon_1 \prod_{j=1}^d p(x_j | \phi_b^\ell) - \epsilon_1 \epsilon_2 \right). \end{aligned}$$

Finally, we take expectations on both sides:

$$\text{MISE}(p, q) \leq 2B^{-2} \mathbb{E} \left[\int_{\mathcal{X}} \alpha^2 + \beta^2 d\mathbf{x} \right],$$

where we have exploited the linearity of expectation to pull the factor outside of the bracketed term, and the monotonicity of expectation to preserve the inequality.

A.2 Proof of Theorem 1

Lemma 1 states that error is bounded by a quadratic function of $\epsilon_1, \epsilon_2, \epsilon_3$. Thus for L_2 -consistency, it suffices to show that $\mathbb{E}[\epsilon_j^2] \rightarrow 0$, for $j \in \{1, 2, 3\}$. Start with ϵ_1 . A general version of the Glivenko-Cantelli theorem [81] guarantees uniform convergence of empirical proportions to population proportions. Let \mathcal{L} denote the set of all possible hyperrectangular subspaces induced by axis-aligned splits on \mathcal{X} . Then we have that $\lim_{n \rightarrow \infty} \sup_{\ell \in \mathcal{L}} |p(\phi^\ell) - q(\phi^\ell)| = 0$ with probability 1.

Next, take ϵ_2 . (A5) guarantees that p satisfies the consistency conditions for univariate KDE [74, 84, 36], while condition (v) of (A4), originally due to Meinshausen [52], ensures that within-leaf sample size increases even as leaf volume goes to zero. Our kernel is a nonnegative function $K : \mathbb{R}^d \rightarrow \mathbb{R}$ that integrates to 1, parametrized by the bandwidth h :

$$p_h(\mathbf{x}) = \frac{1}{nh} \sum_{i=1}^n K\left(\frac{\mathbf{x} - \mathbf{x}_i}{h}\right).$$

Using standard arguments, we take a Taylor series expansion of the MISE and minimize the *asymptotic* MISE (AMISE):

$$\text{AMISE}(p, p_h) = (nh)^{-1} R(K) + \frac{1}{4} h^4 \mu_2(K)^2 R(p''),$$

where

$$\begin{aligned} R(K) &= \int K(x)^2 dx, \\ \mu_2(K) &= \int x^2 K(x) dx, \text{ and} \\ R(p'') &= \int p''(x)^2 dx. \end{aligned}$$

For example values of these variables under specific kernels, see [84, Appx. B]. Under (A5), it can be shown that

$$\text{MISE}(p, p_h) = \text{AMISE}(p, p_h) + o((nh)^{-1} + h^4).$$

Thus if $(nh)^{-1} \rightarrow 0$ and $h \rightarrow 0$ as $n \rightarrow \infty$, the asymptotic approximation is exact and $\mathbb{E}[\epsilon_2^2] \rightarrow 0$.

Finally, take ϵ_3 . The expected square of this value goes to zero if and only if the joint distribution of predictors within each leaf factorizes as a product of marginals, in which case our URF f has fully converged. Thus our goal in this section is to prove the consistency of this algorithm. The consistency of RF classifiers has been shown under various assumptions about splitting rules and stopping criteria [13, 8, 9, 71], but these results generally require trees to be grown to purity or even completion (i.e., $n_b^\ell = 1$ for all ℓ, b). This would of course make intra-leaf density estimation impossible. Moreover, when the overlap assumption (A3) holds, trees can only be grown to purity on pain of overfitting. We therefore follow Malley et al. [50] in observing that regression procedures constitute probability machines, since $\mathbb{P}(Y = 1|\mathbf{x}) = \mathbb{E}[Y|\mathbf{x}]$ for $Y \in \{0, 1\}$.

The honesty and regularity conditions originally introduced by Wager and Athey [83]—subsequently generalized by Athey et al. [3] and further studied by Peng et al. [61]—are well-suited to our task. They provide consistency criteria for regression forests that apply to RF classifiers as a special case when predictions are made via soft labeling. For full details, we refer readers to the original texts. We simply summarize the most pertinent results below, which involve the bias-variance decomposition of RF predictions. Under (A1)-(A4), bias decays at the following rate [83, Thm. 3.2]:

$$|\mathbb{E}[f(\mathbf{x})] - \eta(\mathbf{x})| = \mathcal{O}\left(n_b^{-\frac{1}{2} \frac{\log((1-\gamma)^{-1})}{\log(\gamma^{-1})} \frac{\pi}{d}}\right).$$

Meanwhile, variance decays according to [83, Appx. C.2]:

$$\mathbb{E}\left[\left[f(\mathbf{x}) - \mathbb{E}[f(\mathbf{x})]\right]^2\right] = \mathcal{O}\left(n_b^{-\frac{\log((1-\gamma)^{-1})}{\log(\gamma^{-1})} \frac{\pi}{d}}\right).$$

Since L_2 error is just the sum of squared bias, variance, and irreducible error terms, any RF classifier satisfying (A1)-(A4) will converge as n grows large. (Note that irreducible error does not concern us here, since large values for this term simply suggest that the input distribution is already “close” to its first-order approximation.) Thus $\mathbb{E}[\epsilon_3^2] \rightarrow 0$ almost surely, and the proof is complete.

B Experiments

Our experiments do not include any personal data, as defined in Article 4(1) of the European Union’s General Data Protection Regulation. All data are either simulated or from publicly available resources such as the University of California Irvine Machine Learning repository [26].

We performed all experiments on a dedicated 64-bit Linux platform running Ubuntu 20.04 with an AMD Ryzen Threadripper 3960X (24 cores, 48 threads) CPU, 256 gigabyte RAM and two NVIDIA Titan RTX GPUs. We used R version 4.1.2 and Python version 3.7.12. Further details on the environment setup are provided in the supplemental code.

B.1 Simulations

The `cassini`, `shapes`, and `smiley` simulations are all available in the `mlbench` R package; the `twomoons` problem is available in the `fdm2id` R package. Default parameters were used throughout, with fixed sample size $n = 1000$.

B.2 Real Data

For benchmarking generative models on real-world data, we use the benchmarking pipeline proposed by Xu et al. [87]. In detail, the workflow is as follows:

1. Load classification datasets used in Xu et al. [87], namely `adult`, `census`, `credit`, `covertypes`, `intrusion`, `mnist12`, and `mnist28`. Note that the type of prediction task does not affect the process of synthetic data generation, so we omit the single regression example (`news`) for greater consistency.
2. Split the data into training and test sets (see Table 2 for details).
3. Train the generative models FORGE (number of trees = 10, minimum node size = 5), CTGAN⁴ (batch size = 500, epochs = 300) and TVAE⁵ (batch size = 500, epochs = 300).
4. Generate a synthetic dataset of the same size as the training set using each of the generative models trained in step (3), measuring the wall time needed to execute this task.
5. Train a set of supervised learning algorithms (see Table 2 for details): (a) on the real training data set (i.e., the *Oracle*); and (b) on the synthetic training datasets generated by FORGE, CTGAN and TVAE.
6. Evaluate the performance of the learning algorithms from step (5) on the test set.
7. For each dataset, average performance metrics (accuracy, F1-scores) across learners. We report F1-scores for the positive class, e.g. ‘>50k’ for `adult`, ‘+50000’ for `census` and ‘1’ for `credit`.

Table 2: Benchmark Setup. Supervised learning algorithms for prediction: (A) Adaboost, estimators = 50, (B) Decision Tree, tree depth for binary/multiclass target = 15/30, (C) Logistic Regression, (D) MLP, hidden layers for binary/multiclass target = 50/100

Dataset	Train/Test Set	Learner	Link to dataset
<code>adult</code> [26]	23k/10k	A,B,C,D	http://archive.ics.uci.edu/ml/datasets/adult
<code>census</code> [26]	200k/100k	A,B,D	https://archive.ics.uci.edu/ml/datasets/census+income
<code>covertypes</code> [10]	481k/100k	A,D	https://archive.ics.uci.edu/ml/datasets/covertypes
<code>credit</code> [85]	264k/20k	A,B,D	https://www.kaggle.com/mlg-ulb/creditcardfraud
<code>intrusion</code> [26]	394k/100k	A,D	http://archive.ics.uci.edu/ml/datasets/kdd+cup+1999+data
<code>mnist12</code> [44]	60k/10k	A,D	http://yann.lecun.com/exdb/mnist/index.html
<code>mnist28</code> [44]	60k/10k	A,D	http://yann.lecun.com/exdb/mnist/index.html

⁴https://sdv.dev/SDV/api_reference/tabular/ctgan.html. MIT License.

⁵https://sdv.dev/SDV/api_reference/tabular/tvae.html. MIT License.

B.3 Run Time

In order to evaluate the run time efficiency of FORGE, we chose to focus on the smallest dataset of the benchmark study in Sect. 5.2, namely `adult`. We (A) drew stratified subsamples and (B) drew covariate subsets. For step (B), the target variable is always included. We select an equal number of continuous/categorical covariates when possible and used all $n = 32,561$ instances. Results in terms of processing time are visualized in Fig. 4.

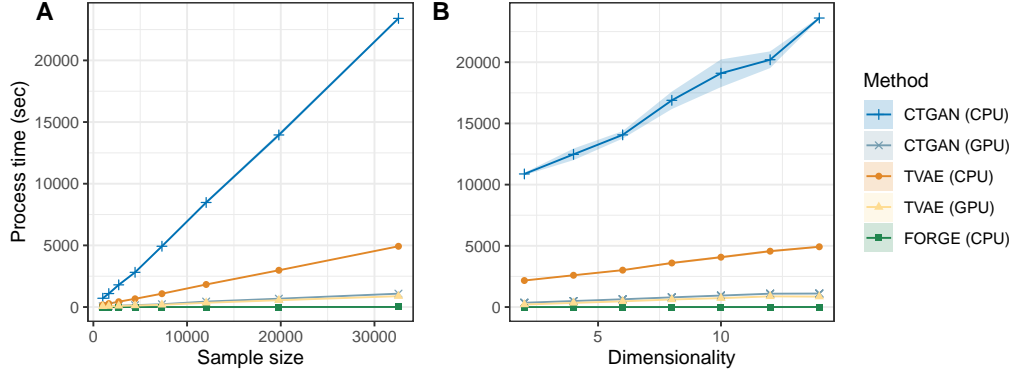


Figure 4: Complexity curves. (A): Processing time as a function of sample size, using stratified subsamples of the `adult` dataset. (B): Processing time as a function of dimensionality, using random features from the `adult` dataset.